J-Researchers

Journal of Civil Engineering Researchers

Journal homepage: www.journals-researchers.com

Groundwater Flow Modeling Using Finite Element Method And Intelligent Aquifer Mesh

Mohammad Javad Zeynali,[a,*] Mohammad Nazeri-Tahroudi [b] , Omolbani Mohammadrezapour,[c]

[a] *Assistant Professor, Department of Water Engineering, University of Torbat Heydarieh, Torbat-e Heydarieh, Iran*
[b] *Asistant Professor, Department of Water Engineering, Lorestan University, Khorramabad, Iran*
[c] *Associate Professor, Department of Water Engineering, Gorgan University of Agricultural Sciences and Natural Resources, Gorgan, Iran*

ABSTRACT

In groundwater flow modeling, as in any modeling problem, a certain amount of error is inevitable. In groundwater flow and contaminant transport modeling, recharge and discharge wells act as point sources or sinks. How these wells are treated can influence accuracy and reduce uncertainty or increase the amount of error. This study investigates an intelligent aquifer mesh. To illastrate the theory, two hypothetical aquifers with triangular and square elements were examined, in both confined and unconfined conditions. In the intelligent aquifer mesh, after gridding the model domain, pumping or recharge wells are considered as nodes. Consequently, the numbering of nodes and elements are updated accordingly. Groundwater flow modeling is performed on the updated mesh to enhance accuracy. The results of this research indicated that considering the recharge and pumping wells as a node and re-gridding the model area can perform groundwater flow modeling with more accuracy and ultimately the results will be more reliable.

ARTICLE INFO

Received: February 02,2026
Accepted: February 28,2026

Keywords:
Aquifer
Finite Element Method
Groundwater Flow Modeling
Intelligent Aquifer Mesh

DOI: 10.61186/JCER.8.1.77
DOR: 20.1001.1.22516530.1399.11.4.1.1

1. Introduction

Groundwater is one of the most important water resources in the world. This resource is particularly critical for inhabitants of arid regions, as their livelihoods depend on it. Therefore, research into the quantity, quality, and management of groundwater resources is of high significance.

Groundwater flow modeling can enhance our understanding of groundwater flow behavior. Additionally, modeling contaminant transport in groundwater provides insights into the movement and dispersion of pollutants within an aquifer over extended timescales, informing remediation strategies. In groundwater modeling, numerical methods such as the finite difference method, the finite element method, and meshless methods are commonly employed. Much research has been conducted in the field of groundwater flow modeling using the finite difference method [1], the finite element method [2], and the meshless method [3]. Numerical methods have also been used in the contaminant transport [4], groundwater remediation [5-7]. To illustrate how numerical methods operate, several studies analyze both hypothetical and real aquifers. Some researchers investigate hypothetical

* Corresponding author. e-mail: mj.zeynali@torbath.ac.ir.

aquifers [8-10] while others examine real aquifers [11] and some have studied both types of aquifers in their research [12,13].

In some plains, the aquifer is recharged by a lake or a wetland, while in others this source of recharge is absent; nevertheless, pumping wells as point discharge sources are present in all plains. In most research on hypothetical or real aquifers, pumping or recharge wells are modeled as point discharge or recharge sources within the model domain. However, in many studies, when examining a hypothetical aquifer, wells are placed exactly on the nodes after regular or irregular gridding of the model dmain [10,14]; in real aquifers, pumping wells are transferred to the nearest node [15,16].

Suppose an aquifer is represented by a square grid with four corner nodes, each side measuring 500 m, and a well placed exactly at the square's center; in this case, the well position can be mapped to any of the four neighboring nodes, which implies a displacement of 354 m. Clearly, transferring the well from one point to another can increase modeling error. Moreover, using a denser grid raises computational cost, and it is not feasible to guarantee that the desired well coincides with a grid node. Consequently, the focus of this research is on developing a intelligent aquifer mesh that, after the initial mesh is created, places pumping or recharge wells exactly on a node by adapting the mesh accordingly; the mesh is updated to ensure a node lies at the well location, and the numbers of nodes and elements are revised before proceeding with the simulation on the new mesh. Hence, the central innovation of this work can be viewed as the intelligentization of finite element gridding, enabling high-accuracy modeling through the strategic addition of pumping or recharge wells.

2. Materials and Methods

In this research, two hypothetical aquifers are investigated to illastrate the theory of intelligent aquifer mesh.

But before examining the performance of numerical models such as finite elements, these models should be validated. For this purpose, the groundwater level for a hypothetical homogeneous and isotropic aquifer reported by Illangasekare, and Doll, (1989) was simulated and compared with the analytical results [17]. The hypothetical aquifer according to Figure 1 has a length of 3200 meters and a width of 2800 meters, and the thickness of the aquifer, Transmissivity and specific yield are 30 m, 885.71 m2/day and 0.15, respectively. The upper and lower boundaries are of the type of boundary with constant head and the left and right boundaries are considered as no-flow boundaries. Also, two pumping wells are located at (1400,1400) and (1400,1800) with flow rates of 1142.85 and 1428.57 m3/day, respectively. There was also an observation well at the coordinates (1000,1000) and the duration of the simulation was considered equal to 210 days.

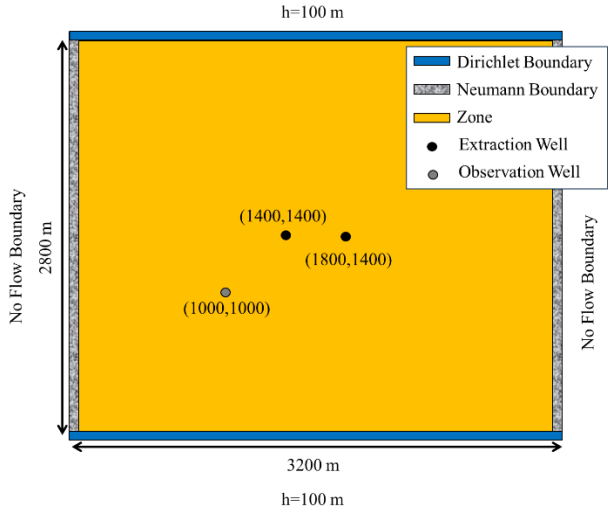

Figure 1. Hypothetical aquifer configuration (Illangasekare, and Doll, (1989))

The model domain is gridded with a density of 200 m by 200 m and the nodes are numbered as shown in Figure 2.

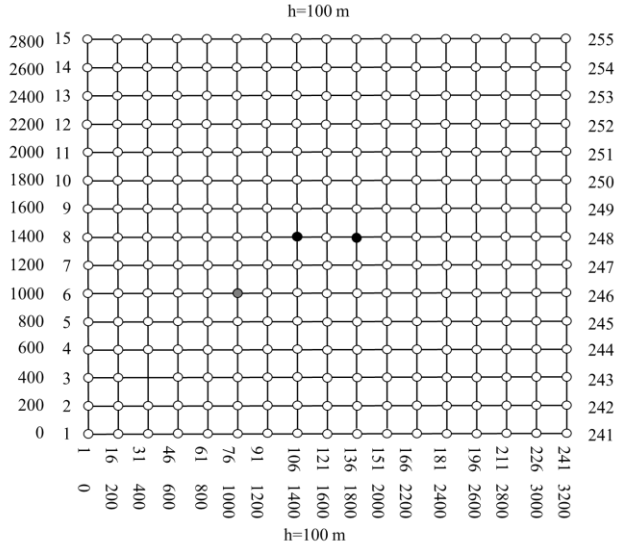

Figure 2. mesh model domain 200m×200m

2.1. Case Study 1

A hypothetical auifer with length of the 1500 and its width equal to 1000 m is considered (Figure 3). The hydrogeologic parameters for the aquifer are presented in Table 1. There is a lake with rate of seepage of 0.02 m/d in

Zone A. Also, top of Zones A and bottom of Zone C are considered to be recharged and discharsed at a rate of 0.2 and -0.2 m/d, respectively. The flow model has constant head conditions on its left and right boundaries with 100 and 98 m, respectively and the other boundares are the no-flow boundary. There are four pumping wells and one recharge well in this hypothetical auifer.

four pumping wells are located on (770,400), (700,650), (1250,350) and (1230,725) coordinate with the rate of pumping of 600, 500, 400 and 300 m3/day respectively and the recharge well is located on (200,200) coordinate with the rate of recharge of 500 m3/day.

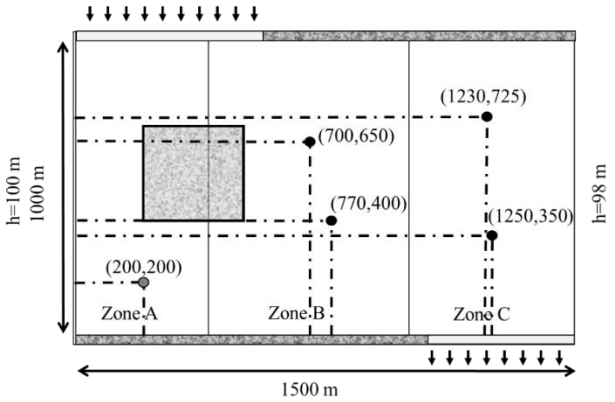

Figure 3. Hypothetical aquifer configuration (First Case Study)

Table 1.
Hydrogeologic data used for flow model (First Case Study)

Properties	Zone A	Zone B	Zone C
Hydrolic Conductivity (Kx)	5	4	3
Hydrolic Conductivity (Kx)	8	5	2
Specific Yield	0.15	0.15	0.15
Aquifer Thickness	100	100	100
Transmissivity (Tx)	500	400	300
Transmissivity (Ty)	800	500	200
Storage Coefficient	0.15	0.15	0.15

We can see three diferent hydrolic conductivity in hypothetical auifer domain. Therefore, we must grid the model domain in such a way that the edges of the elements coincide with the boundary between the two zones. Considering this issue, the gridding was done in such a way that nodes 1 to 55 were placed in Zone A, nodes 56 to 121 in Zone B, and nodes 122 to 176 in Zone 3. Also, considering this type of gridding, the lake boundary located in Zone A corresponds to nodes 27 to 30, 38 to 41, 49 to 52, and 60 to 63. Figure 4 shows rectangular (square) gridding of the model domain. As can be seen in this figures, one of the wells (recharge well) is located exactly on node number 25, but the other wells are not exactly coinside on the nodes. Also, the inflow to the aquifer occurs from the boundary of Zone A and from nodes 22, 33, 44, 55, and 66, and the outflow from the aquifer occurs from the boundary of Zone C and from nodes 122, 133, 144, and 155. The inflow and outflow rates are 0.2 and 0.01 m/day, respectively.

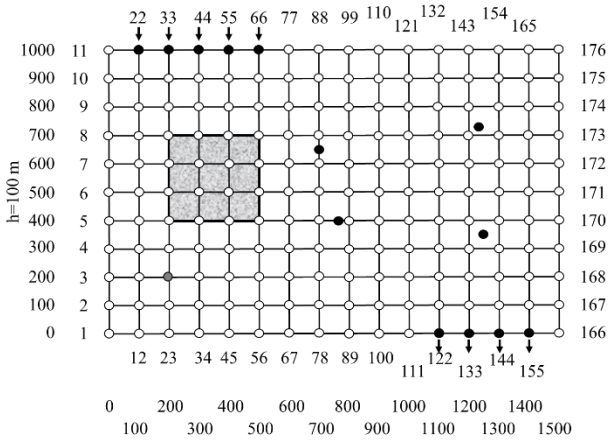

Figure 4. Rectangular mesh of the model domain (First Case Study)

2.2. Case Study 2

A second hypothetical auifer with length of the 800 and its width equal to 600 m is considered (Figure 5). The hydrogeologic parameters for the aquifer are presented in Table 2. There is a lake with rate of seepage of 0.02 m/d in this aquifer. Also, part of right side and part of bottom of aquifer are considered to be recharged and discharsed at a rate of 0.2 and -0.2 m/d, respectively. The flow model has constant head conditions on its other boundaries with 80 m, respectively. There are three pumping wells in this hypothetical auifer.

Three pumping wells are located on (220,110), (470,470) and (670,380) coordinate with the rate of pumping of 300, 200 and 100 m3/day respectively.

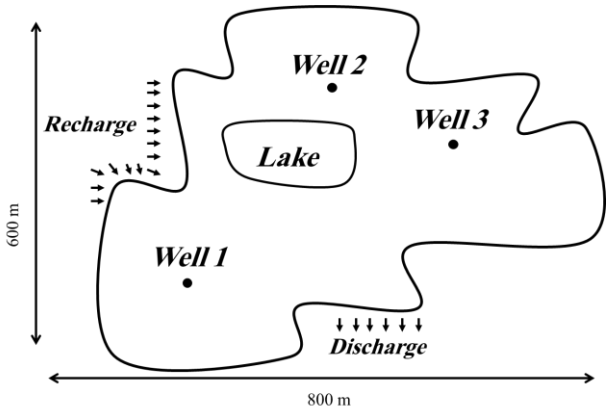

Figure 5. Hypothetical aquifer configuration (Second Case Study)

Table 2.
Hydrogeologic data used for flow model (Second Case Study)

Properties	
Hydrolic Conductivity (Kx)	5
Specific Yield	0.15
Aquifer Thickness	100
Transmissivity (Tx)	500
Storage Coefficient	0.15

Figure (6-a) shows rectangular (square) gridding that covers the entire aquifer domain.

In this figure, elements within the model domain are shown in white and elements outside the model domain are shown in gray.

As can be seen in this figure, the left boundary of the constructed mesh does not coincide with the lower left boundary of the aquifer. In other words, we could have deleted the elements of the first column from the left. However, this column of elements was intentionally placed so that the lack of effect of elements outside the model boundary can be clearly seen in the modeling.

In Figure (6-b) all of node are numbered. As can be seen in this figures, three pumping wells are not exactly coinside on the nodes. Also, the inflow to the aquifer occurs from the left side boundary and from nodes 11, 18, 19, and 20, and the outflow from the bottom side boundary and from nodes 37, and 44. The inflow and outflow rates are 0.01 and 0.01 m/day, respectively.

2.3. Intelligent mesh

In the intelligent mesh, we consider the wells as nodes. Therefor, number of nodes and elements will be changed. The Figure 7 and Fig. 8 show the triangular and rectangular gridding of the model domain. In this hypothetical aquifer, after the triangular intelligent mesh, the node number does not change, and the four wells that are not located exactly on the node are assigned node numbers 177 to 180. However, the number and order of the elements change. this triangular intelligent mesh can be implemented using Delaunay triangulation.The recharge well in the new rectangular mesh located on node 31. Also, the inflow to the aquifer occurs from the boundary of Zone A and from nodes 28, 42, 56, 70, and 84, and the outflow from the aquifer occurs from the boundary of Zone C and from nodes 169, 183, 197, 211, 225 and 239.

As mentioned before, In the intelligent mesh, we consider the wells as nodes. Therefor, number of nodes and elements will be changed. Figure (9-a) shows the rectangular gridding of the entire domain that we considered. Also, Figure (9-b) shows the rectangular gridding of the only model domain. according to the intelligent mesh, pumping well location and recharge and discharge flow from boundaries must be updated. Therefor, in new mesh pumping well located on node 17, 50 and 73. Also, the inflow to the aquifer occurs from the left boundary side and from nodes 5, 10, 11, 12, 13, and 14, and the outflow from bottom boundary of the aquifer occurs from nodes 53, and 62.

Also, the lake, which is the aquifer recharge and which we have considered as an distributed source, is placed in elements 32, 33, 34, 42, 43, and 44, according to the conventional numbering of the elements.

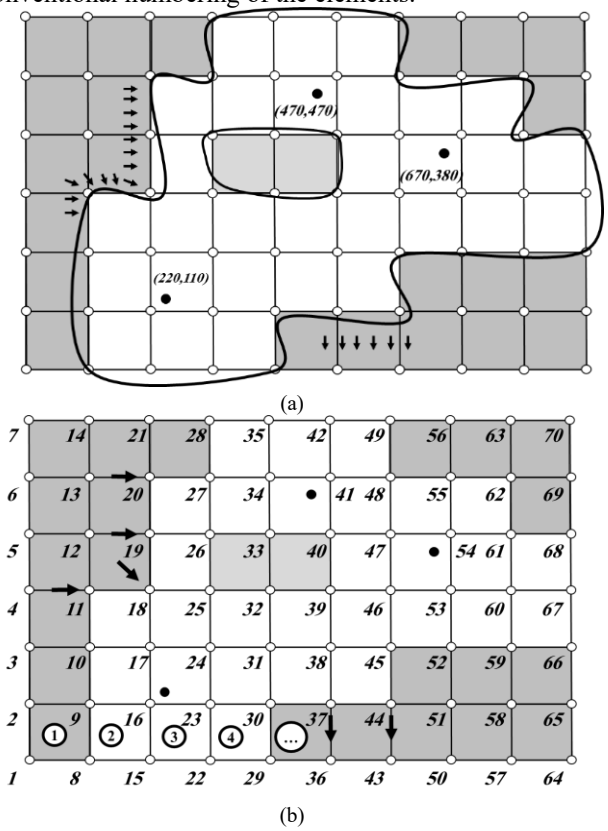

Figure 6. Hypothetical aquifer configuration (Second Case Study)

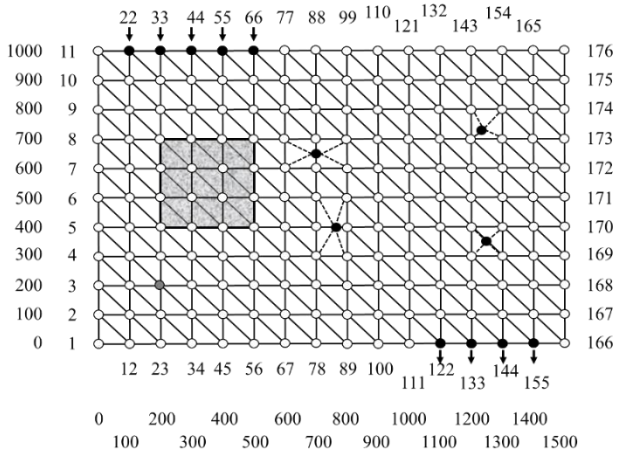

Figure 7. Intelligent triangular mesh of the model domain (First Case Study)

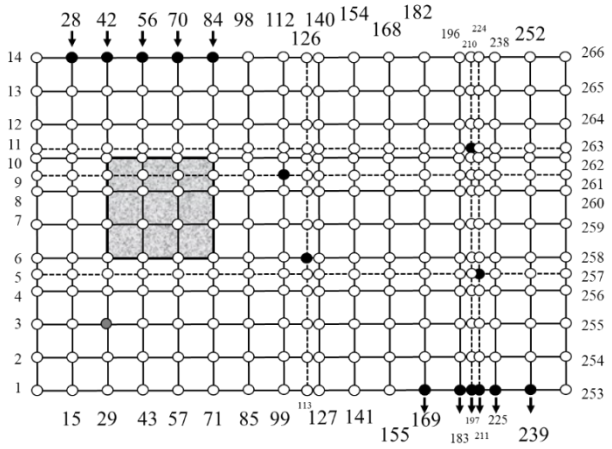

Figure 8. Intelligent rectangular mesh of the model domain (First Case Study)

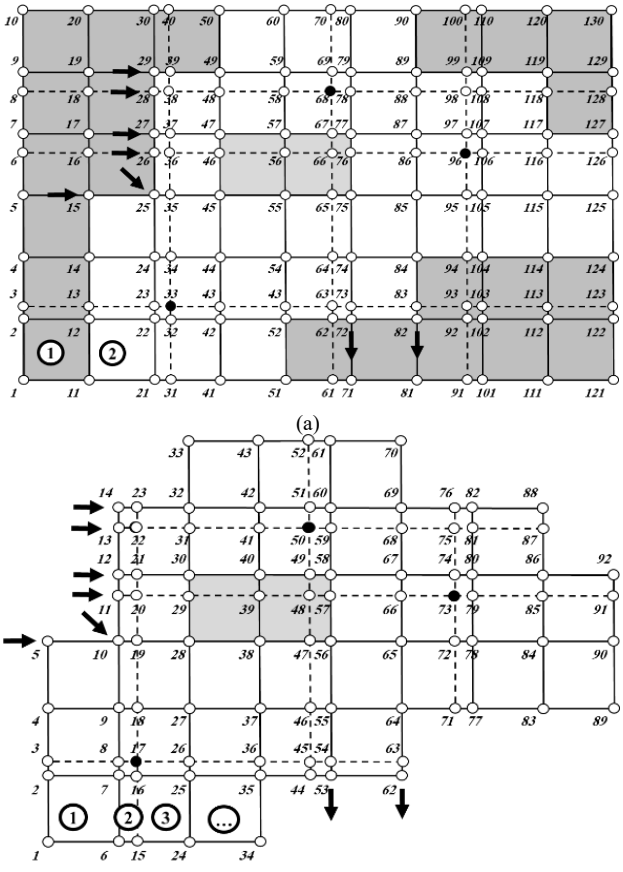

Figure 9. Intelligent rectangular mesh of the model domain (Second Case Study)

In the Intelligent triangular mesh, pumping well located on node 17, 50 and 73. Also, the inflow to the aquifer occurs from the left boundary side and from nodes 5, 10, 11, 12, 13, and 14, and the outflow from bottom boundary of the aquifer occurs from nodes 53, and 62.

Also, the lake, which is the aquifer recharge and which we have considered as an distributed source, is placed in elements 63, 64, 65, 66, 67, 68, 83, 84, 85, 86, 87, and 88, according to the conventional numbering of the elements. Figure (10-a) shows the triangular gridding of the entire domain that we considered. Also, Figure (10-b) shows the triangular gridding of the only model domain.

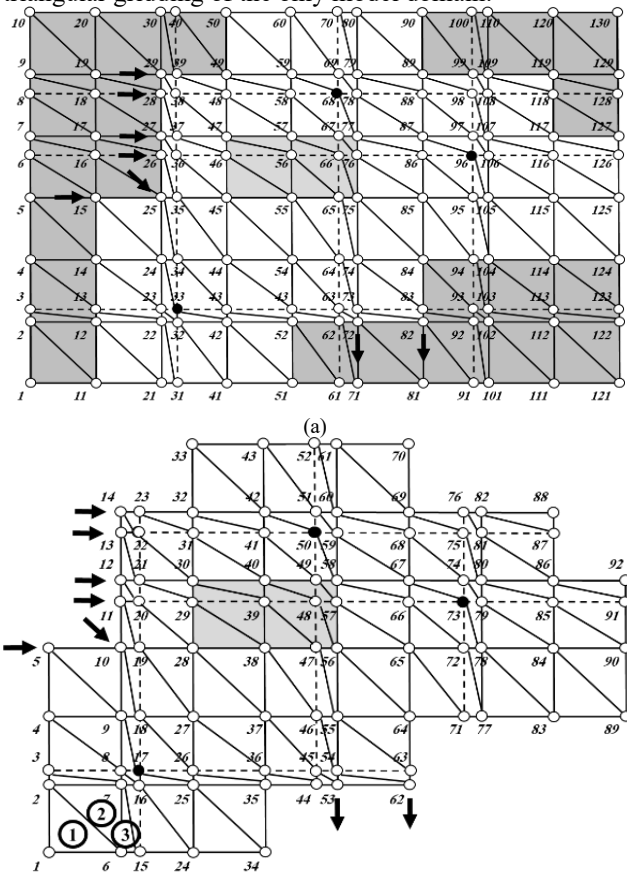

Figure 10. Intelligent triangular mesh of the model domain (Second Case Study)

2.4. The Steps of intelligent mesh

The intelligent aquifer mwsh is performed in several general steps, and the image created in each step is shown in Figure 11.

Step 1: Create a regular distribution of nodes that cover the entire aquifer domain and have specific x and y coordinates.

Step 2: Identifying elements that are inside and outside the boundary, as well as nodes that are inside, on, or outside the model domain boundary,

Step 3: Detecting nodes where boundary flow occurs and elements that experience extended distributed sources.

Step 4: Inserting wells where x and y coordinates are specified.

Step 5: Update the number of nodes, elements and their retransition numbers. Also boundary nodes with inflow and outflow and elements with distributed sources.

Step 6: Extraction of the model domain mesh and its modeling.

Groundwater flow modeling using intelligent mesh can be examined in three general parts. The details of each part are explained in detail below:

Part One: Data Input and Initial Processing

1- Importing model data

1-1- Creating a regular distribution of nodes

1-2- Conventional numbering of nodes

1-3- Specifying the x and y coordinates of nodes

1-4- Specifying boundary nodes, inside nodes and outside nodes of the model domain

1-5- Specifying the values of hydrogeological parameters for nodes located on the boundary and inside the model domain

1-6- Specifying the inflow and outflow values for nodes affected by the inflow and outflow on boundary

1-7- Specifying the distributed sources values for nodes affected by the distributed sources

1-8- Specifying the x and y coordinates of pumping and recharge wells and their pumping or recharge rate values

2- Specifying the nodes of each element

2-1- Specifying the nodes of each element in the overall aquifer domain

2-2- Specifying the nodes of each element in the aquifer domain

Part Two: Updating Nodes and Elements

1- Checking the compliance or non-compliance of the wells and nodes (wells that do not coincide are considered one node)

2- Passing horizontal and vertical lines through new nodes

3- Identifying the intersection of horizontal and vertical lines with the edges of the old mesh

4- Extracting unique nodes and removing common nodes

5- Updating the number of elements and nodes of each element based on the newly added nodes

6- Updating elements that have distributed sources

7- Updating nodes that have inflow or outflow

8- Calculating the values of hydrogeological parameters for new nodes based on neighboring nodes

9- Orderly arrangement of nodes around the model boundary in a vector

Part Three: Groundwater Flow Modeling

1- Initialization and Calculations

1-1- Initialization

1-2- Construction of Stiffness matrices and unsteady flow matrices

1-3- Construction of boundary flow vector

1-4- Construction of distributed sources matrix

1-5- Construction of point sources matrix

2- Groundwater flow modeling and storage

3- Displaying results through graphs

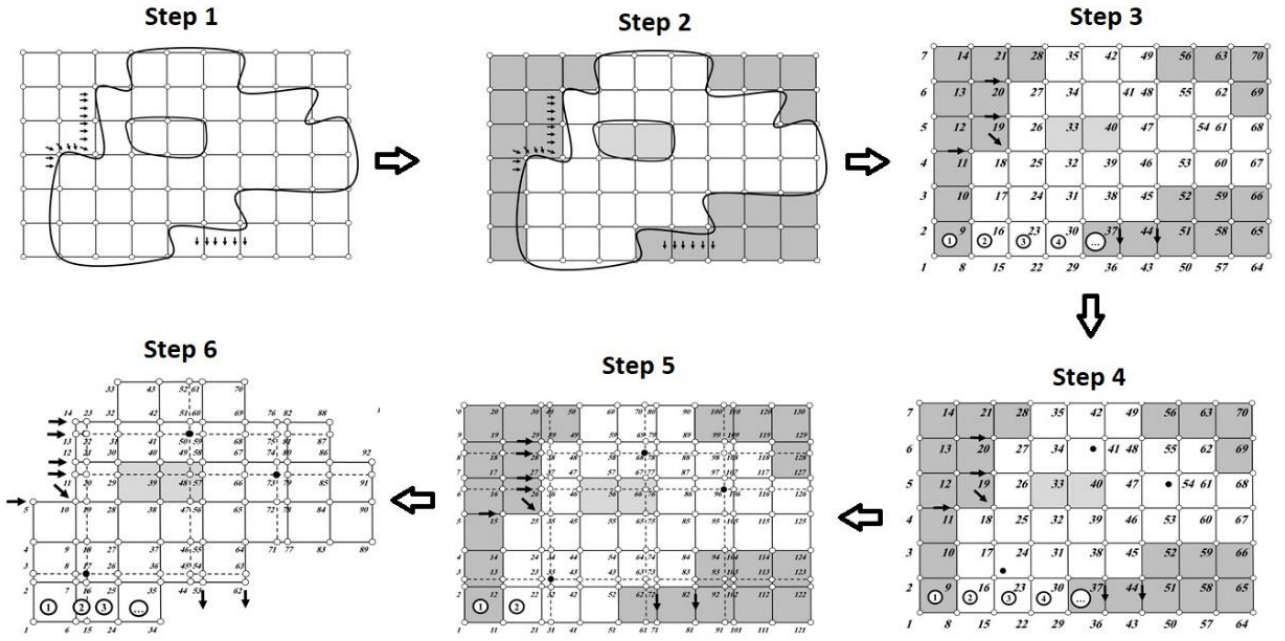

Figure 11. Flowchart of intelligent mesh

3. Results and Discussion

3.1. Validation of numerical model

To implement the finite element model to solve this problem, a time period of one day ( ) was considered and the Crank-Nicholson method ( ) was used. The comparison of finite element numerical method with analytical values in Illangasekare, and Doll, (1989) aquifer is shown in Figure 12 and the head area is shown in Figure 13. According to the values of SSE and RMSE performance criteria, which are 0.0420 and 0.0141, respectively, the results indicated that the performance of the finite element method for groundwater flow modeling has been accepted and is in agreement with the research results of Kulkarni, (2015) and Jafarzadeh, et al. (2021) is consistent [18,19].

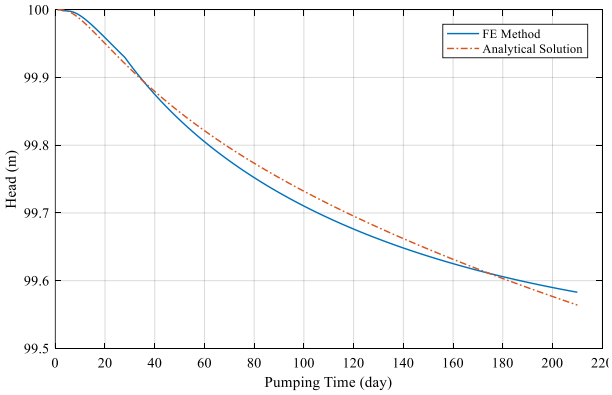

(a)

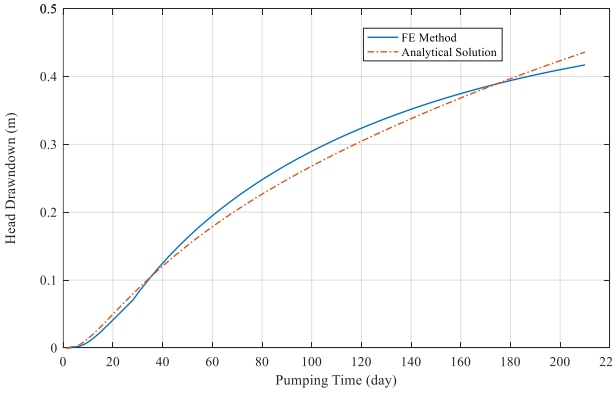

(b)

Figure 12. Head and head drowdown after 210 days

Also, a summary of the performance of the finite element method for this problem considering the time interval of 0.1 days ($\Delta t = 0.1$) and Crank-Nicholson method ($\alpha = 0.5$) is given in table 3.

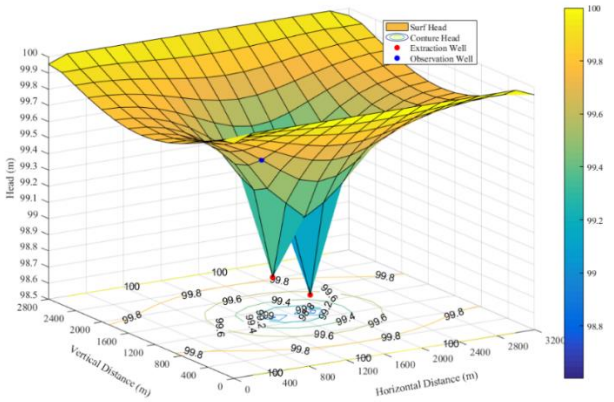

Figure 13. Head in model domain

3.2. The Results of Case Study 1

The first hypothetical aquifer has been investigated using finite element. The results of groundwater flow modeling in confident and unconfident aquifer for 5 years by intelligent triangular mesh are presented in Figure 14 and Figure 15, respectivly.

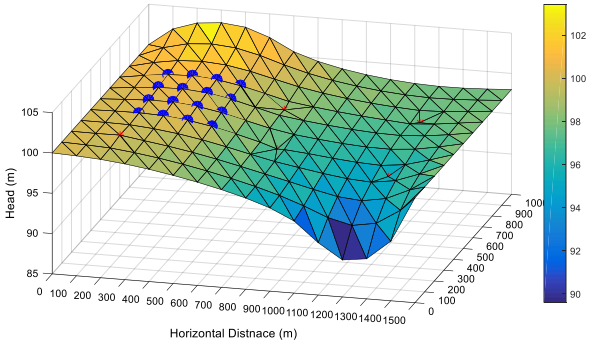

(a) Triangular Mesh – 3D View

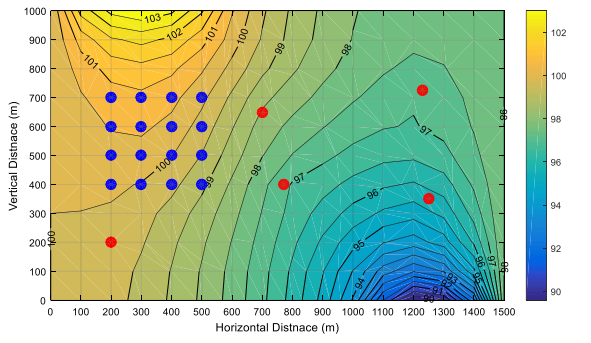

(b) Triangular Mesh – Contour

Figure 14. Groundwater head in confident aquifer in case study 1

Table 3.
summary of the performance of the finite element method

mesh density	Performance Criteria in $\Delta t = 1$		Computational cost (seconds)	Performance Criteria in $\Delta t = 0.1$		Computational cost (seconds)
50 m × 50 m	rmse	0.0996	216.9655	rmse	0.0138	2130.88
	mse	0.0099		mse	0.00019	
	sse	2.0837		sse	0.0401	
100 m × 100 m	rmse	0.0837	8.6195	rmse	0.0306	98.4415
	mse	0.0011		mse	0.0009	
	sse	0.2236		sse	0.1967	
200 m × 200 m	rmse	0.0141	0.3788	rmse	0.0404	6.0545
	mse	0.0002		mse	0.0016	
	sse	0.0420		sse	0.3422	
400 m × 400 m	rmse	0.1720	0.0895	rmse	0.1589	1.5062
	mse	0.0296		mse	0.0253	
	sse	6.2094		sse	5.3054	

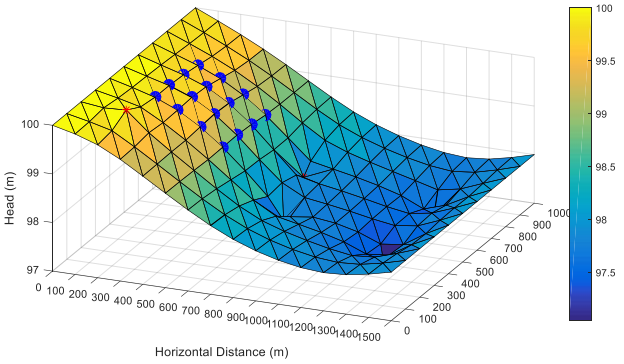

(a) Triangular Mesh – 3D View

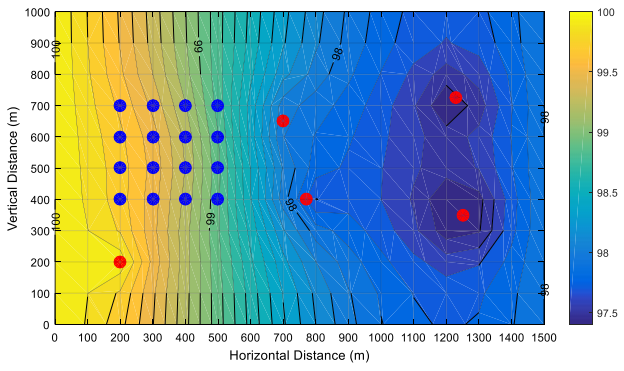

(b) Triangular Mesh – Contour

Figure 15. Groundwater head in confident aquifer in case study 1

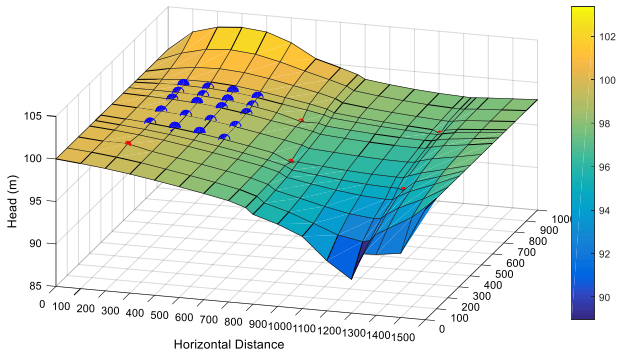

(a) Triangular Mesh – 3D View

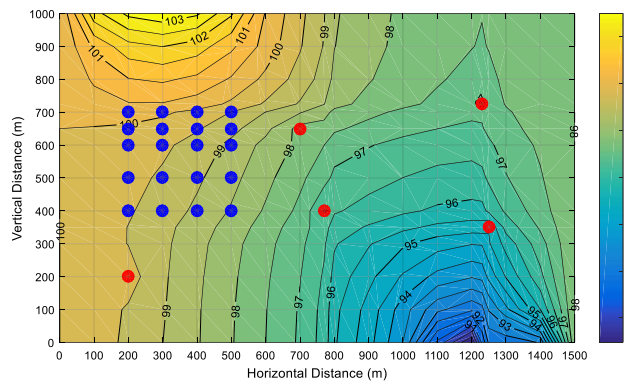

(b) Triangular Mesh – Contour

Figure 16. Groundwater head in confident aquifer in case study 1

The results of groundwater flow modeling in confident and unconfident aquifer for 5 years by intelligent rectangular mesh are presented in Fig. (16) and Fig. (17), respectivly.

3.3. The Results of of Case Study 2

The second hypothetical aquifer has been investigated using finite element. The results of groundwater flow modeling in confident and unconfident aquifer for 5 years

by intelligent triangular mesh are presented in Figure (18) and Figure (19), respectivly.

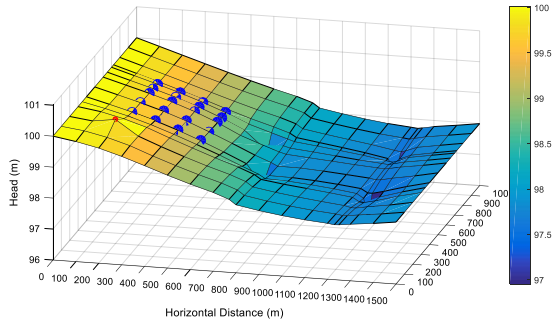

(a) Triangular Mesh – 3D View

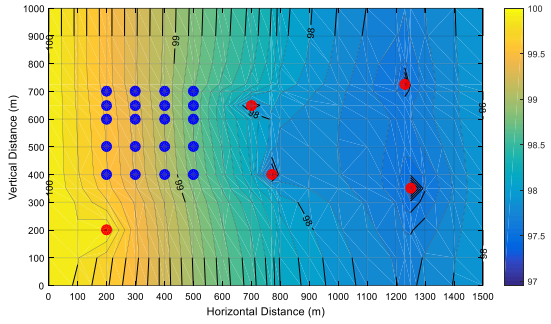

(b) Triangular Mesh – Contour

Figure 17. Groundwater head in unconfident aquifer in case study 1

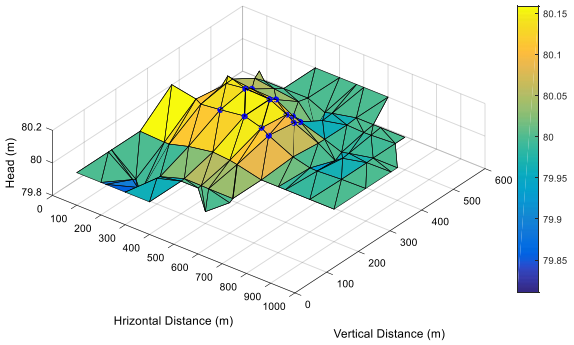

(a) Triangular Mesh – 3D View

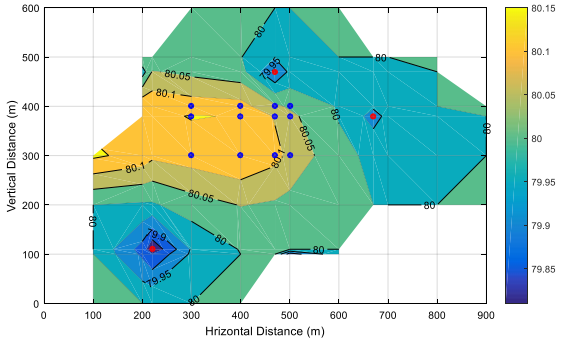

(b) Triangular Mesh – Contour

Figure 18. Groundwater head in confident aquifer in case study 2

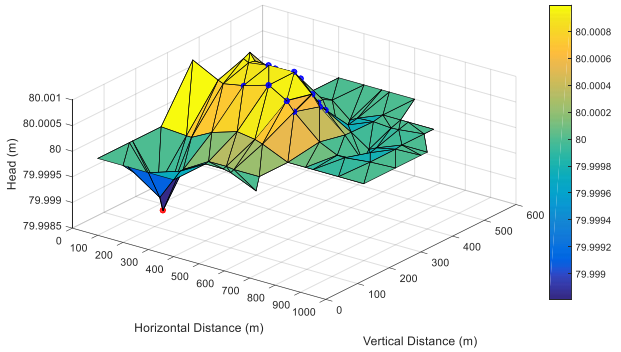

(a) Triangular Mesh – 3D View

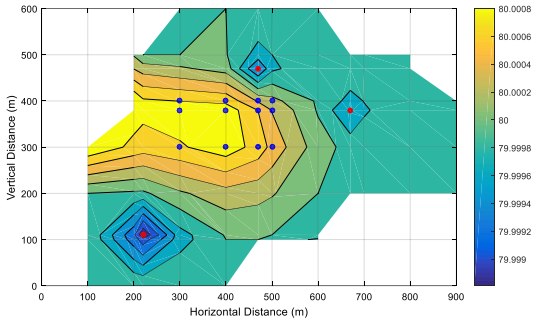

(b) Triangular Mesh – Contour

Figure 19. Groundwater head in unconfident aquifer in case study 2

The results of groundwater flow modeling in confident and unconfident aquifer for 5 years by intelligent rectangular mesh are presented in Figure 20 and Figure 21, respectivly.

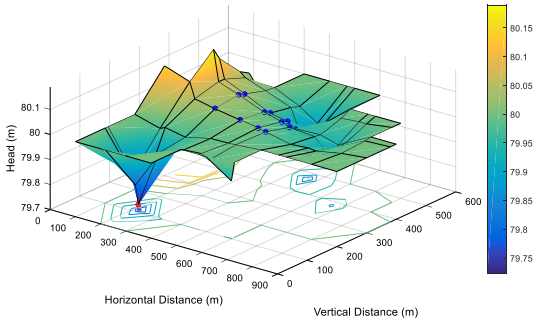

(a) Triangular Mesh – 3D View

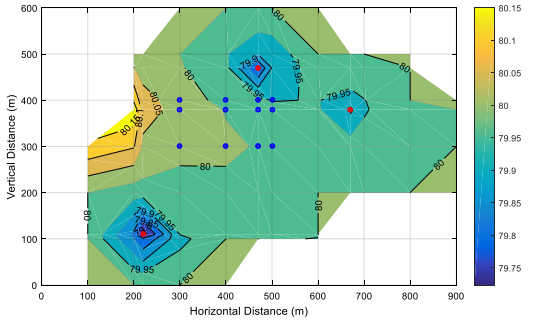

(b) Triangular Mesh – Contour

Figure 20. Groundwater head in confident aquifer in case study 2

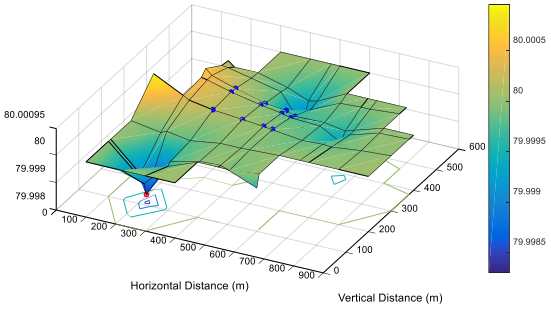

(a) Triangular Mesh – 3D View

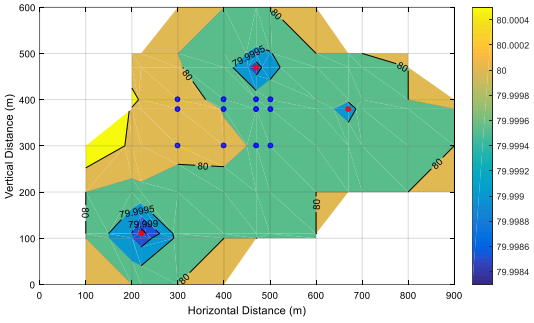

(b) Triangular Mesh – Contour

Figure 21. Groundwater head in unconfident aquifer in case study 2

Also, Head value in the nearest neighboring node of wells for confident and unconfident aquifer for case study 1, presented in Table 4.Also, Head value in the nearest neighboring node of wells for confident and unconfident aquifer for case study 2, presented in Table 5.As can be seen in Figure 2, nodes 140, 141, 151, and 152 are at the same distance from well number 4, but the difference between the triangular and square element modeling in the confined aquifer according to Table 3 is greater than the other three nodes with a value of 0.1844. The reason for this can be attributed to the existence of a boundary with the outflow at the bottom of the aquifer. However, in the case of well number 3 at nodes 136 and 148, the difference between the triangular and square element modeling is greater than the other two nodes with values of 0.6751 and 0.3185, respectively. This is also true for well numbers 1 and 2 in the second hypothetical aquifer. The difference between the triangular and square element modeling in the confined aquifer according to Table 4 is greater than the other nodes with values of 0.9395 and 0.1386 at nodes 24 and 33. In the case of unconfined aquifer, the difference between triangular and square element modeling in the unconfined aquifer, according to Table 4, with values of 0.0004 and 0.0008, is greater in nodes 24 and 33 than in other nodes.

Table 4.
Head value in the nearest neighboring node for case study 1

Well	Node Number	confident aquifer		unconfident aquifer			
		Triangular Mesh	Rectangular Mesh	Triangular Mesh	Rectangular Mesh		
		Col (1)	Col (2)	Col (3)	Col (4)	Col (5)= abs(Col (1)-Col (2))	Col (6)= abs(Col (3)-Col (4))
W0	25	100.0001	99.7319	99.7995	99.8786	0.2682	0.0791
W1	82	97.6312	97.3785	98.5028	98.6657	0.2527	0.1629
	93	96.9477	96.5566	98.2846	98.3932	0.3911	0.1086
W2	84	98.2736	97.8836	98.5141	98.6448	0.3900	0.1307
	85	98.6387	98.5416	98.5458	98.6922	0.0971	0.1464
W3	136	95.1976	94.5225	97.9592	98.0881	0.6751	0.1289
	137	95.9412	95.8376	97.9923	98.0764	0.1036	0.0841
	147	95.6327	95.6957	97.8102	97.9063	0.0630	0.0961
	148	96.2669	96.5854	97.9318	97.9035	0.3185	0.0283
W4	140	97.0602	97.0744	98.0682	98.0548	0.0142	0.0134
	141	97.3769	97.3620	98.1059	98.0658	0.0149	0.0401
	151	97.2670	97.4514	98.0317	97.9797	0.1844	0.0520
	152	97.4759	97.5915	98.0565	97.9851	0.1156	0.0714

Table 5.
Head value in the nearest neighboring node for case study 2

Well	Node Number	confident aquifer		unconfident aquifer			
		Triangular Mesh	Rectangular Mesh	Triangular Mesh	Rectangular Mesh		
		Col (1)	Col (2)	Col (3)	Col (4)	Col (5)= abs(Col (1)-Col (2))	Col (6)= abs(Col (3)-Col (4))
W1	16	79.8901	79.8516	79.9993	79.9990	0.0385	0.0003
	17	79.9923	79.9722	80.0000	79.9998	0.0201	0.0002
	23	79.9584	79.9339	79.9997	79.9996	0.0245	0.0001
	24	79.0263	79.9658	80.0002	79.9998	0.9395	0.0004
W2	33	80.1196	79.9810	80.0007	79.9999	0.1386	0.0008
	34	80.0019	79.9536	80.0000	79.9997	0.0483	0.0003
	40	80.0424	79.9475	80.0003	79.9997	0.0949	0.0006
	41	79.9679	79.9161	79.9998	79.9995	0.0518	0.0003
W3	46	80.0145	79.9682	80.0001	79.9998	0.0463	0.0003
	47	79.9955	79.9519	80.0000	79.9997	0.0436	0.0003
	53	79.9875	79.9699	79.9999	79.9998	0.0176	0.0001
	54	79.9690	79.9483	79.9998	79.9997	0.0207	0.0001

Therefore, in general, it can be said that the further the well location is from the surrounding nodes, the greater the difference between modeling with triangular and square elements. These results indicated that the smaller the distance between the nodes and the well location, the more accurate the results obtained will be. This requires increasing the mesh density, which will increase the computational cost, or another approach should be adopted, for which the use of a intelligent mesh can be considered a suitable option.

4. Conclusion

In the modeling of groundwater flow and contaminant transport, numerical methods such as finite difference and finite elements (triangular and rectangular elements) are used. In these modelings, whether the aquifer is hypothetical or real, there are always recharge or discharge wells as point source or sink. In dealing with this point source, a simple approach is to transfer the recharge or discharge well to the nearest node after gridding the model area. In this case, if several wells are close to a node, they all coincide on that node and finally their pumping rates are summed together. Beside, to avoid such a discrepancy, smaller regular mesh can be used to ensure that all wells coincide on the nodes. However, it is obvious that using small mesh increases the computational cost. Therefore, in this study, a different mesh was used in dealing with pumping wells. In this approach, after gridding the model domain, pumping or recharge wells are considered as nodes. and the numbering of nodes and elements is changed and updated accordingly, so that groundwater flow modeling can be done more efficiently and accurately. In this study, two hypothetical aquifer were investigated and an attempt was made to include all the characteristics of an aquifer, such as different hydraulic conductivity in different parts of the aquifer, application of distributed source and point source and sink, boundary conditions of a specific head (Dirichlet condition), a specific and no-flow boundary (Neuman condition). The results of this research indicated that considering the recharge and pumping wells as a node and re-gridding the model area can perform groundwater flow modeling with more accuracy and ultimately the results will be more reliable.

5. Acknowledgment

This work has been financially supported by the University of Torbat Heydarieh. The grant number is UTH: 1404/08/17-271.

6. Declarations

Conflict of interest None.Competing interests The authors declare that they have no known competing financial interests or personal relationships that could have appeared to influence the work reported in this paper.

References

[1] Chávez-Negrete C, Domínguez-Mota FJ, Román-Gutiérrez R (2024). Interface formulation for generalized finite difference method for solving groundwater flow. Computers and Geotechnics. 166, 105990. https://doi.org/10.1016/j.compgeo.2023.105990

[2] Akbarpour A, Zeynali MJ, Tahroudi MN (2020). Locating optimal position of pumping Wells in aquifer using meta-heuristic algorithms and finite element method. Water Resources Management, 34(1), 21-34. https://doi.org/10.1007/s11269-019-02386-6

[3] Singh KG, Pathania T (2025). Development and real field application of meshless generalized finite difference method for unconfined groundwater flow modelling. Mathematics and Computers in Simulation. https://doi.org/10.1016/j.matcom.2024.108855

[4] Zeynali MJ, Pourreza-Bilondi M, Akbarpour A, Yazdi J, Zekri S (2022). Optimizing pump-and-treat method by considering important remediation objectives. Applied Water Science. 12(12): 268. https://doi.org/10.1007/s13201-022-01782-5

[5] Zeynali MJ, Nazeri Tahroudi M, Mohammadrezapour O (2024). Optimizing Pump-and-Treat Method by Using Optimization-Simulation Models. Sustainable Earth Trends. 4(3): 19-30. https://doi.org/10.48308/set.2024.236332.1060

[6] Zeynali MJ, Nazeri Tahroudi M, Mohammadrezapour O (2024). Investigating the Optimization-Simulation Problem of Groundwater Remediation Under Various Scenarios. Water Harvesting Research. 7(1): 125-139. https://doi.org/10.22077/jwhr.2024.7158.1099

[7] Kumar D, Ch S, Mathur S, Adamowski J (2015). Multi-objective optimization of in-situ bioremediation of groundwater using a hybrid metaheuristic technique based on differential evolution, genetic algorithms and simulated annealing. Journal of Water and Land Development, 27(1), 29-40. https://doi.org/10.1515/jwld-2015-0016

[8] Mategaonkar M, Eldho TI, Kamat S (2018). In-situ bioremediation of groundwater using a meshfree model and particle swarm optimization. Journal of Hydroinformatics, 20(4): 886-897. https://doi.org/10.2166/hydro.2018.110

[9] Guneshwor L, Eldho TI, Kumar AV (2018). Identification of Groundwater Contamination Sources Using Meshfree RPCM Simulation and Particle Swarm Optimization. Water Resources Management, 32(4): 1517-1538. https://doi.org/10.1007/s11269-017-1889-8

[10] Mohtashami A, Akbarpour A, Mollazadeh M (2017). Development of two-dimensional groundwater flow simulation model using meshless method based on MLS approximation function in unconfined aquifer in transient state. Journal of Hydroinformatics, 19(5), 640-652. https://doi.org/10.2166/hydro.2017.005

[11] Eldho TI, Swathi B (2018). Groundwater contamination problems and numerical simulation. Environmental Contaminants: Measurement, Modelling and Control, 167-194. https://doi.org/10.1007/978-981-10-7332-8_8

[12] Ghafouri HR, Darabi BS (2007). Optimal identification of ground-water pollution sources. International Journal of Civil Engineering, 5(2), 144-156. https://doi.org/10.1007/s40999-007-0014-3

[13] Sharief SMV, Eldho TI, Rastogi AK, Gurunadha Rao VVS (2012). Optimal groundwater remediation by pump and treat using FEM-and EGA-based simulation-optimization model. Journal of Hazardous, Toxic, and Radioactive Waste. 16(2): 106-117. https://doi.org/10.1061/(ASCE)HZ.2153-5515.0000097

[14] Zeynali MJ, Pourreza-Bilondi M, Akbarpour A, Yazdi J, Zekri S (2022). Development of a contaminant concentration transport model for sulfate-contaminated areas. Applied Water Science. 12(7): 169. https://doi.org/10.1007/s13201-022-01689-1

[15] Zeynali MJ, Nazeri Tahroudi M, Mohammadrezapour O (2025). Groundwater Flow Modeling and Adopting a Different Approach in Dealing Pumping Wells. Water Harvesting Research, 8(2), 284-298. https://doi.org/10.22077/jwhr.2025.10542.1195

[16] Illangasekare TH, Döll P (1989). A discrete kernel method of characteristics model of solute transport in water table aquifers. Water Resources Research, 25(5), 857–867. https://doi.org/10.1029/WR025i005p00857

[17] Kulkarni NH (2015). Numerical simulation of groundwater recharge from an injection well. International Journal of Water Resources and Environmental Engineering, 7(5), 75-83. https://doi.org/10.5897/IJWREE2015.0584

[18] Jafarzadeh A, Pourreza-Bilondi M, Akbarpour A, Khashei-Siuki A, Samadi S (2021). Application of multi-model ensemble averaging techniques for groundwater simulation: synthetic and real-world case studies. Journal of Hydroinformatics, 23(6), 1271-1289. https://doi.org/10.2166/hydro.2021.058